Application note

Monitoring enzyme kinetics using UV-Visible absorption spectroscopy

Michaelis-Menten analysis

Introduction

In biological systems, enzymes will act as a catalyst, increasing the rate of a biochemical reaction.[1–3] These reactions span a large variety of different functions in nature, including metabolic mechanisms and energy storage within cells.[2] In these reactions, the precursor, commonly referred to as the "substrate," will bind to an active site on the enzyme. Following complexation, the product will be released, leaving behind the free enzyme (Figure 1). As the ability for a compound to bind to an enzyme is highly dependent on structure, there will be a small subset of molecules which can interact with the active site, making enzymes highly selective for specific reaction mechanisms.[3]

$$E + S \rightleftharpoons ES \longrightarrow E + P$$

Figure 1: General reaction scheme for enzyme-catalyzed product formation.

In the pharmaceutical applications spaces, some developed drugs take advantage of the structural requirements to aid in specific enzymatic pathways where a deficiency may exist, much like adenosine deaminase (ADA), a material which can treat immunodeficient individuals.[4] Conversely, other pharmaceutical products are developed to block some enzymatic pathways, such as the formation of melanin in the body.[5] Similarly, many food products inherently include enzymes which can participate in reactions which degrade the material over time. Food scientists will investigate these reactions to understand the kinetic mechanism and work on pathways to mitigate the formation of unwanted side products. As such, it is important to understand the reaction kinetics and competing pathways which can affect the overall reaction.

The reaction rate, also referred to as the velocity of the reaction, is dependent on the concentration of the substrate. As substrate concentration increases, the reaction rate will also increase. However, at very high concentrations, the rate of the reaction will no longer change as most of the active sites will be filled, following typical binding equilibria (Figure 2). The change in reaction rate as a function of substrate concentration has been well characterized and, in many cases, can be modeled through the Michaelis-Menten equation,

$$v = \frac{V_{max}[S]}{K_m + [S]} \quad (1)$$

in which v is the rate of the reaction, $[S]$ is the substrate concentration, V_{max} is the maximum rate, and K_m is the Michaelis constant.[1]

Through fitting the calculated initial reaction rates as a function of substrate concentration to the Michaelis-Menten equation, both V_{max} and K_m can be determined (Figure 2). Not only does this type of analysis give information about the maximum possible rate, but it also sheds light on the required reaction conditions through the Michaelis constant. K_m defines the concentration at which half of the active sites are filled by the substrate.[1] With this information, the minimum substrate concentration needed to effectively synthesize the final product can be found, allowing for a better understanding of the optimal reaction conditions.

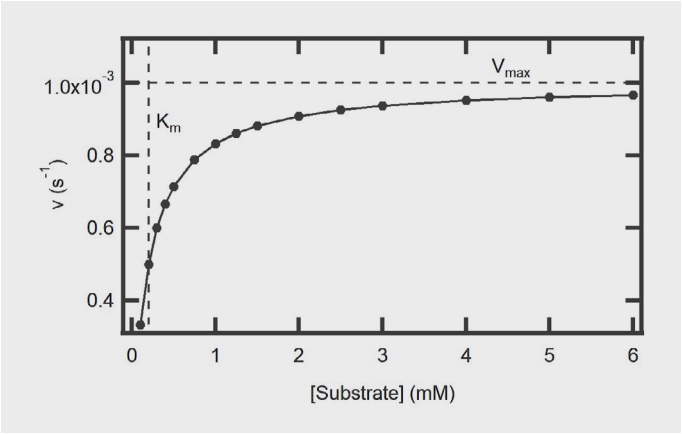

Figure 2: Example of a Michaelis-Menten plot. The vertical line refers to K_m, while the horizontal line corresponds to V_{max}.

As enzyme-based reactions involve the formation of an enzyme-substrate complex, there are circumstances under which a secondary compound, an inhibitor, may interact with the enzyme prior to complex formation. This secondary compound may inhibit the enzyme-substrate reaction pathway by introducing a side reaction pathway, changing the enzyme-substrate reaction rates as a result. Consequently, it is important to understand the nature by which the inhibitor affects the reaction between the enzyme and substrate, as this information can be used to determine methods for preventing side reactions.

There are multiple different forms of inhibition which can occur in an enzymatic system. First, an inhibitor can be competitive, in which the compound will bind to the active site, preventing the substrate from reacting with the enzyme as expected (Figure 3a).[1,6,7] This form of inhibition can involve a compound with a similar structure as the substrate or a chelating agent, allowing for association to the active site on the enzyme.[6,7] In this system, K_m will be higher than if the inhibitor were not present as, according to Le Chatelier's principle, a higher substrate concentration is needed to favor the formation of the enzyme-substrate complex.[1] Additionally, V_{max} will exhibit no change as, at higher substrate concentrations, the formation of the enzyme-substrate complex is favored and will match the rates found for systems in which no inhibitor is present.[1,6]

The Lineweaver-Burk plot can be used to visualize the effect inhibition has more easily on the reaction rates as a function of substrate concentration. This form of analysis involves plotting the inverse of the reaction rate as a function of the inverse of the substrate concentration.[1,8] This effectively linearizes the Michaelis-Menten equation, as shown in equation 2.

$$\frac{1}{v} = \frac{1}{V_{max}} + \frac{K_m}{[S]*V_{max}} \qquad (2)$$

By the nature of the Lineweaver-Burk analysis, the V_{max} and K_m values extrapolated will be less accurate than the values determined by fitting the data to the Michaelis-Menten equation, considering error propagation by transforming *v* and *[S]* to *1/v* and *1/[S]*.[9] However, the changes observed in the Lineweaver-Burk plot as inhibitor concentration increases can be used to confirm the type of inhibition exhibited in the system. For competitive inhibition, the slope of the Lineweaver-Burk plot is expected to increase compared to the system containing no inhibitor (Figure 3b).[8] However, as V_{max} is not expected to deviate with and without an inhibitor present, the y-intercept should match.[8]

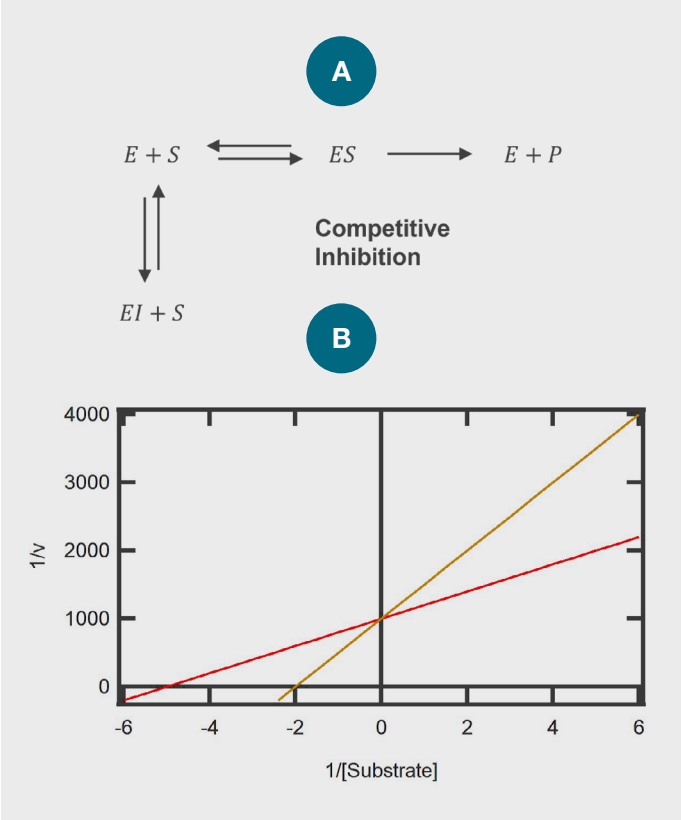

Figure 3: (a) General reaction mechanism and (b) Lineweaver-Burk plot for competitive inhibition.

For the second form of inhibition, the inhibitor and substrate can both bind to different active sites on the enzyme (noncompetitive, Figure 4a). Under these circumstances, the inhibitor may be bulky, preventing the substrate from binding to the active site of the enzyme when bound, or the bound inhibitor prevents the product from detaching from the enzyme.[1,6] In noncompetitive inhibition, V_{max} is expected to be lower as the enzyme-inhibitor complex cannot react with the substrate, effectively lowering the concentration of "active" enzymes in solution. However, K_m is not expected to change as higher concentrations of substrate cannot change the binding equilibrium between the enzyme and the inhibitor.[6] A typical Lineweaver-Burk plot for noncompetitive inhibition will exhibit an increase in the slope of the line as a function of inhibitor concentration. As V_{max} will be lower, the y-intercept should be higher, however, the x-intercept will remain the same, as shown in Figure 4b.[8]

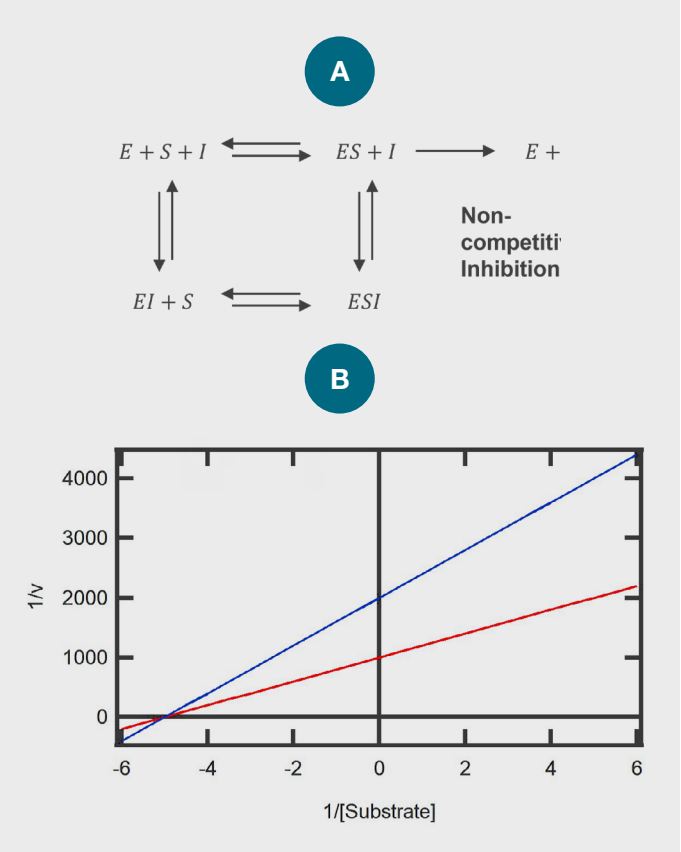

Figure 4: (a) General reaction mechanism and (b) Lineweaver-Burk plot for noncompetitive inhibition.

Third, the inhibitor only reacts with the enzyme-substrate complex, preventing the formation of the product (uncompetitive inhibition, Figure 5a).[6,10] Following Michaelis-Menten analysis, the uncompetitive inhibitor system will have both a lower V_{max} as the secondary reaction pathway competes with the desired pathway, lengthening the time it takes to form the product. Additionally, K_m will decrease as the formation of the product is less favorable.[5] When linearized in the Lineweaver-Burk plot, the slope for the uncompetitive inhibitor system will match, however, the Y-intercept will be higher (Figure 5b).[10]

One of the many methods that can be employed to follow enzyme kinetics uses UV-Visible absorption spectroscopy.[11] Given the product or substrate absorbs in the UV-Visible spectral region, the absorbance can be monitored as a function of time. According to Beer's law,

$$A = cl\varepsilon \qquad (3)$$

where A is absorbance, c is concentration, l is path length, and ε is molar absorptivity, absorbance is linearly proportional to concentration. Consequently, monitoring changes in absorbance will linearly reflect changes in the concentration of the absorptive compound. As this technique is nondestructive, the final product can be further analyzed after the kinetics experiment is completed.

Herein, we demonstrate the ability to follow enzymatic reactions using the Thermo Scientific™ Evolution™ One Plus Spectrophotometer. The tyrosinase-catalyzed reaction with catechol in the presence and absence of an inhibitor (kojic acid) was used as a model system. Reaction rates were determined within the Thermo Scientific Insight™ Pro Software for each reaction assay run, assuming a zeroth order reaction rate. From the calculated rates, a Michaelis-Menten analysis was performed, allowing for the determination of both V_{max} and K_m in the presence of varying inhibitor concentrations. In addition, Lineweaver-Burk plots were constructed as well, and the inhibition by kojic acid was found to be competitive in nature.

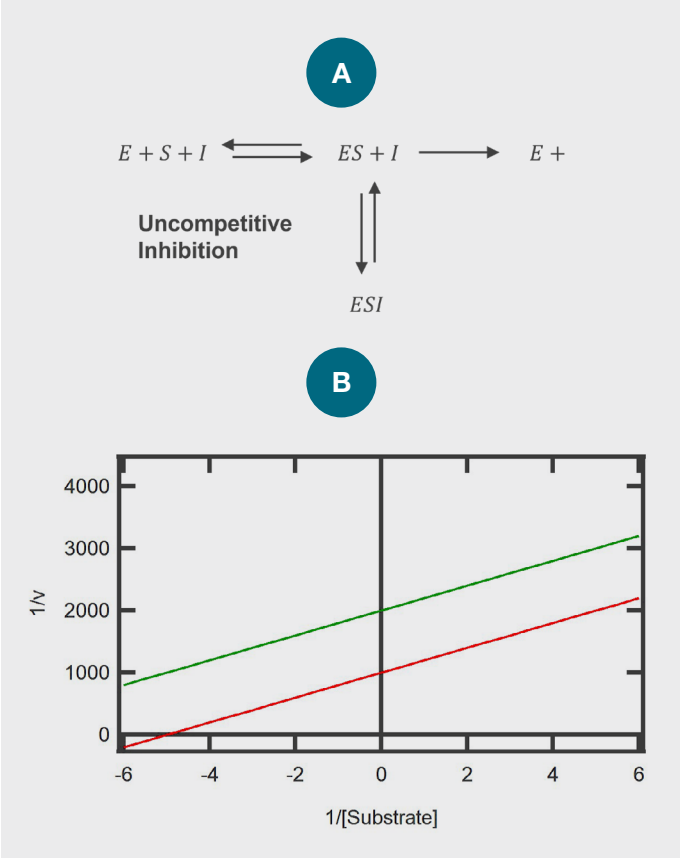

Figure 5: (a) Reaction mechanism and (b) Lineweaver-Burk for uncompetitive inhibition.

Experimental

Mushroom tyrosinase

In these experiments, tyrosinase was extracted from a mushroom and reacted with catechol based on the procedure defined by Flurkey et al.[12] 1.1 g of mushrooms were ground and mixed in 10 mL of 10 mM dihydrogen phosphate (phosphate buffer) to produce a stock solution of tyrosinase extract. The solution was then decanted to remove large mushroom pieces and filtered using a 0.22 µm hydrophilic syringe filter (PDVF). The resulting solution appeared transparent and pink/brown in color and will be referred to as the tyrosinase extract in this text. A 10 mM stock catechol solution was made using 0.5 mM o-phosphoric acid, while a 2.0 mM kojic acid stock solution was also made using deionized water.

The inhibitor-free kinetic assays were then prepared by diluting 125 µL of the tyrosinase extract with 10 mM phosphate buffer, deionized water, and 10 mM catechol to achieve 5 assays (Table 1) with varying catechol concentration (0.33 mM, 0.67 mM, 1.7 mM, 3.3 mM and 5.0 mM catechol). The final phosphate buffer concentration was 0.2 mM for each assay. A blank solution was also made, containing no tyrosinase extract, catechol, or kojic acid. For the kinetics assays which contained an inhibitor, the same procedure was followed (Table 1), except 50 and 100 µL of 2 mM kojic acid were added to each solution.

Kinetics Assay Set	Volume of 10 mM catechol (mL)	Volume of 2 mM kojic acid (µL)	Total reaction volume (mL)
No inhibitor	0.75	0	1.5
	0.50		
	0.25		
	0.10		
	0.050		
67 µM inhibitor present	0.75	50	
	0.50		
	0.25		
	0.10		
	0.050		
130 µM inhibitor present	0.75	100	
	0.50		
	0.25		
	0.10		
	0.050		

Table 1: Starting material volumes used for each kinetic assay run.

The absorbance at 410 nm of each solution was collected as a function of time with a the Evolution One Plus Spectrophotometer using a 1.0 nm spectral bandwidth. The data was collected every 20 seconds for 5 min using a 10 mm plastic cuvette. The integration and dwell times were each set to 0.5 seconds. For each assay, the reaction rate was determined using the data collected in the first 150 seconds using the Analyze function in the Insight Pro Software, assuming a zeroth order reaction rate. The Michaelis-Menten and Lineweaver-Burk plots were constructed and fit to the appropriate equation in a separate software.

Spectral scans were collected for the mushroom extract (125 µL of stock solution diluted to 1.5 mL of solution using phosphate buffer), 2.0 mM kojic acid, 10 mM catechol, and the final reaction mixture in the presence of kojic acid (130 µM) and catechol (5.0 mM). Each sample was held in a plastic 10 mm cuvette and measured every 2.0 nm between 350 nm and 800 nm. The data was integrated 0.11 seconds at each data interval, and a 1.0 nm spectral bandwidth was used.

Results and discussion

Tyrosinase is a naturally occurring compound found in the human body as well as in a variety of plant-based products.[5, 12–14] In humans, this enzyme participates in a reaction with L-3,4-dihydroxyphenylalanine (L-DOPA) in the presence of oxygen, forming dopaquinone which can further polymerize through the quinone group, leading to the formation of melanin.[7] As shown in Figure 6, L-DOPA includes a catechol moiety which participates in the polymerization reaction. As such, tyrosinase can similarly react with catechol alone to form a structurally similar product (Figure 6c).[12] Both reactions follow traditional Michaelis-Menten kinetics, and the final products for both mechanisms can be monitored using UV-Visible absorption techniques.

Figure 7a includes the absorbance collected at 410 nm from the first 150 seconds for each reaction run with no inhibitor included. This analysis wavelength was chosen as catechol, kojic acid, and the tyrosinase extract do not absorb at 410 nm while the reaction product does (Figure 7b). As mentioned previously, the time-based absorption measurements were fit to a zeroth order reaction rate using the Insight Pro Software, removing the need for manual fitting procedures. These fits were not attempted at longer reaction times as the reaction had begun to slow, deviating from a linear curve due to the loss of the rate-limiting reagent. As expected, increasing the concentration of the substrate, catechol, increases the rate of the reaction, however, at concentrations higher than 1.7 mM, the reaction rate changes minimally (Table 2).

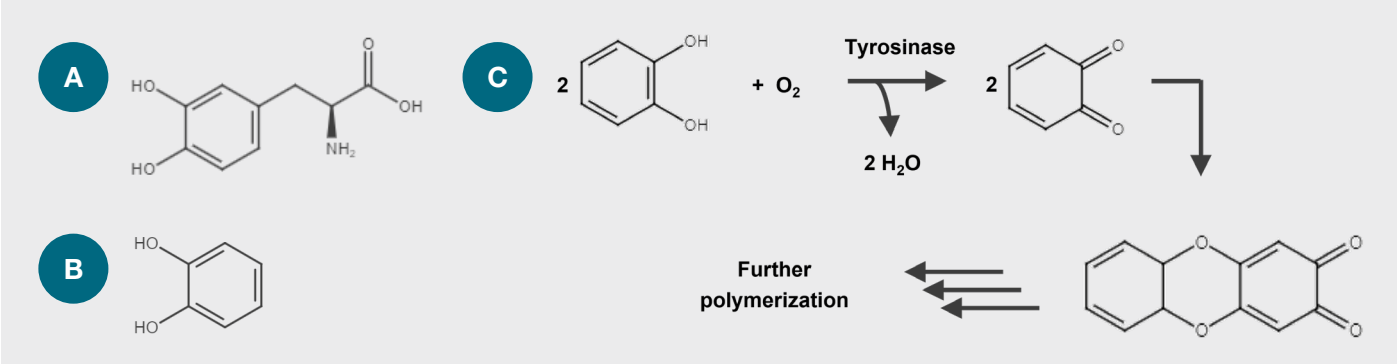

Figure 6: Chemical structure for (a) L-DOPA and (b) catechol. (c) General reaction mechanism for the catechol polymerization reaction catalyzed by tyrosinase.

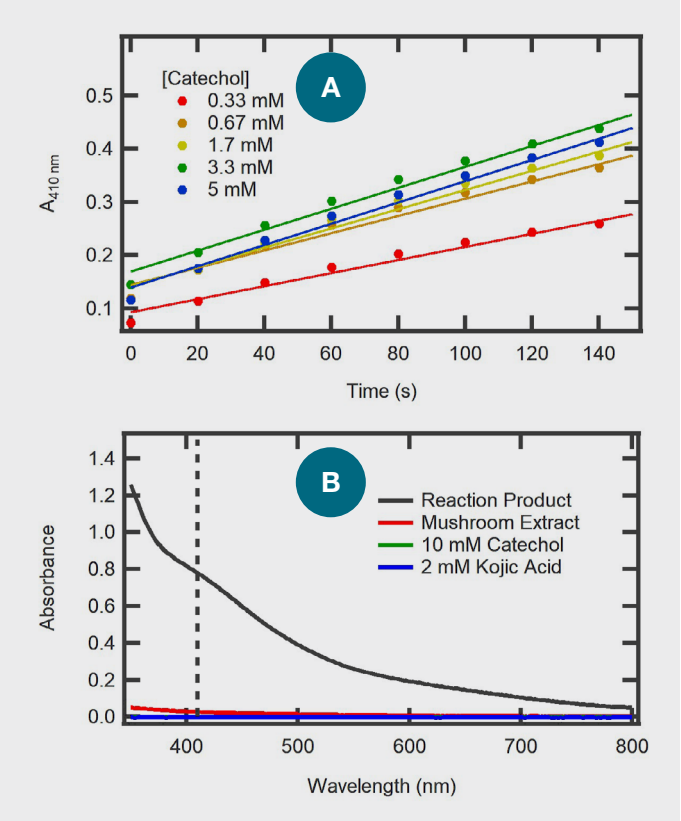

Figure 7: (a) Absorption at 410 nm as a function of reaction time for mushroom tyrosinase samples in the presence of 0.33 mM (red), 0.67 mM (orange), 1.7 mM (yellow), 3.3 mM (green) and 5.0 mM (blue) catechol. Each data was fit to a linear function in the first 150 s to determine the rate of each reaction. (b) Absorption spectra for the reaction product (black line), mushroom extract (red line), 10 mM catechol (green line), and 2.0 mM kojic acid (blue line). The dashed line indicates the analysis wavelength used for the absorption measurements collected as a function of time.

Catechol concentration (mM)	Rate (s^{-1})
0.33	0.0012
0.67	0.0015
1.7	0.0017
3.3	0.0019
5.0	0.0019

Table 2: Reaction rates calculated using the Insight Pro Software for each catechol concentration used.

The Michaelis-Menten kinetics analysis was then used to determine the maximum reaction rate, as well as the Michaelis constant. As shown in Figure 8, the rates of the tyrosinase-catechol reaction are plotted as a function of catechol concentration, resulting in a curve which fits well to the Michaelis-Menten equation (equation 1). Through the fitting procedure, the maximum reaction rate (V_{max}) and the Michaelis constant (K_m) were found to be 0.00198 s^{-1} and 0.219 mM, respectively (Table 3).

While understanding the reaction mechanism and rates for an enzymatic reaction are highly important, it can also be equally important to understand the effects an inhibitor plays on the reaction rate. In the tyrosinase-catechol reaction, kojic acid (Figure 9a) can act as an inhibitor.

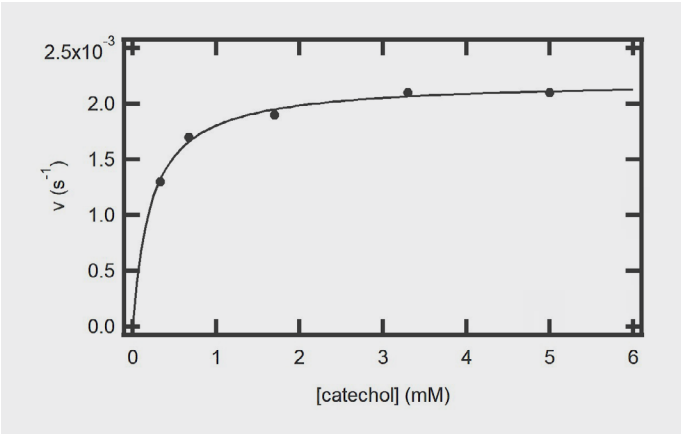

Figure 8: Michaelis-Menten plot demonstrates the changes in rate constants as a function of catechol concentration. The line represents the fit curve constructed using the Michaelis-Menten function.

Kojic acid concentration (µM)	K_m (mM)	V_{max} (s^{-1})
0	0.219 ± 0.02	0.00198 ± 0.00003
67	1.1 ± 0.1	0.00175 ± 0.00008
130	2.2 ± 0.3	0.0018 ± 0.0001

Table 3: K_m and V_{max} values determined through Michaelis-Menten analysis (equation 1).

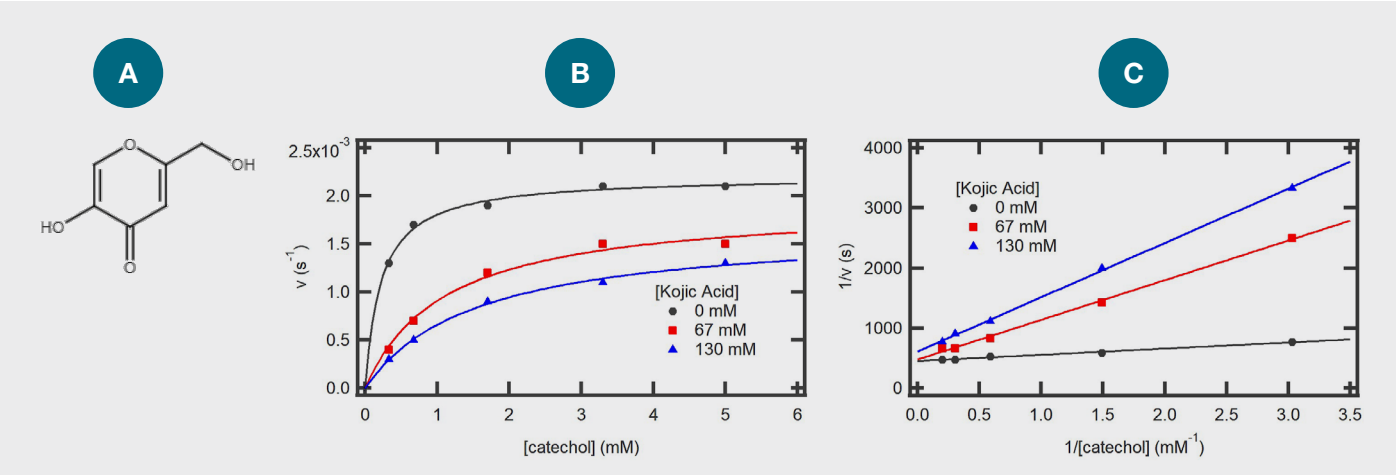

Figure 9: (a) Chemical structure for kojic acid. (b) Michaelis-Menten and (c) Lineweaver-Burk plots for the tyrosinase-catechol reaction in the presence of 0 µM (black circles), 67 µM (red squares), and 130 µM (blue triangles) kojic acid.

As such, the same enzyme assays were prepared as previously done, however, these samples were prepared with 67 µM and 130 µM kojic acid as described in the experimental section.

As with the samples measured without kojic acid, the reaction rates for the tyrosinase-catechol reaction in the presence of 67 µM and 130 µM kojic acid still increase with increasing concentration of catechol. However, the reaction rates are slower as kojic acid acts as an inhibitor for this enzymatic reaction. Following Michaelis-Menten kinetic analyses for both data sets (Figure 9b), K_m was found to increase with increasing concentration of kojic acid. The increase in K_m suggests more catechol is needed to effectively compete with kojic acid. Additionally, the similar V_{max} indicates the effect of the inhibitor can be overcome with a high concentration of catechol present. As described previously, these changes to K_m and the similarity in V_{max} suggest kojic acid is acting as a competitive inhibitor.

The linearized form of the Michaelis-Menten plot, Lineweaver-Burk, can be used as well to better visualize the effect an inhibitor has on an enzymatic reaction. Figure 9c includes the plot of 1/[catechol] vs. 1/v. Here, the data is fit to a linear function. It was observed that the presence of kojic acid results in an increase in the slope of the Lineweaver-Burk plot, while the y-intercept was found to be similar in all the data sets (Table 4). The x-intercept of the Lineweaver-Burk plot, $1/K_m$, increases as the kojic acid concentration increases (Table 4). This behavior further confirms that kojic acid acts as a competitive inhibitor, in agreement with literature.[7] This is likely due to the similar structural motifs between catechol and kojic acid, leading to kojic acid binding to the active site in place of catechol.

Kojic acid concentration (µM)	Slope K_m/V_{max} (mM•s)	Y-intercept $1/V_{max}$ (s)	X-intercept $1/K_m$ (mM^{-1})
0	108 ± 5	507 ± 8	-4.7 ± 0.8
67	640 ± 20	540 ± 30	-0.84 ± 0.6
130	1480 ± 50	430 ± 80	-0.30 ± 0.05

Table 4: Slope, y-intercept, and x-intercept for the Lineweaver-Burk linear fitting functions.

Conclusion

Herein, the Evolution One Plus was used to follow the tyrosinase-catechol reaction using tyrosinase extracted from mushrooms. The rates of the reactions were calculated through the Insight Pro Software and plotted as a function of catechol concentration. Following Michaelis-Menten analysis, the maximum reaction rate (V_{max}) as well as the Michaelis constant (K_m) were determined to be 0.00198 ± 0.00003 s^{-1} and 0.219 ± 0.02 mM, respectively. In the presence of kojic acid, the reaction rates were found to decrease, indicating kojic acid inhibits the formation of the polymerized product. From the Michaelis-Menten fitting parameters, the maximum reaction rate was found to remain the same while the Michaelis constant increased, suggesting kojic acid acts as a competitive inhibitor. This implies higher concentrations of catechol can shift the equilibrium towards favoring product formation.

The experiments described herein demonstrate the ability to use UV-Visible absorption techniques to readily determine enzymatic reaction rates through non-destructive means. While this technique is limited to reactants and products which absorb in the UV-Visible region, the information gleaned in this analysis can help define optimal reaction conditions to favor the formation of a desired product. Additionally, the effect on the reaction kinetics due to the presence of an inhibitor can be investigated through this analysis. With this information, details about the inhibition mechanism, as well as potential methods for mitigating unwanted side reactions, can be explored.

References

1. Berg, J.M.; Tymoczko, J.L.; Stryer, L., Enzymes: Basic Concepts and Kinetics. In *Biochemistry*, 5th ed.; W.H. Freeman and Company, **2002**, 189–225.
2. Ulusu, N.N., Evolution of Enzyme Kinetic Mechanisms, *J. Mol. Evol.*, **2015**, 80, 251–257.
3. Mateo, C.; Palomo, J.M.; Fernandez-Lorente, G.; Guisan, J.M., Fernandez-Lafuente, R., *Enzyme Microb.* Technol., **2007**, 40, 1451–1463.
4. Meghwanshi, G.K.; Kaur, N.; Verma, S.; Dabi, N.K.; Vashishtha, A.; Charan, P.D.; Purohit, P.; Bhandari, H.S.; Bhojak, N.; Kumar, R., Enzyme for Pharmaceutical and Therapeutic Applications, *Biotechnol. Appl. Biochem.*, **2020**, 4, 586–601.
5. Hashim, F.J.; Vichitphan, S.; Han, J.; Vichitphan, K., Alternative Approach for Specific Tyrosinase Inhibitor Screening: Uncompetitive Inhibition of Tyrosinse by *Moringa oleifera, Molecules*, **2021**, 26, 4576.
6. Amine, A.; Mohammadi, H.; Bourais, I.; Palleschi, G., Enzyme Inhibition-based Biosensors for Food Safety and Environmental Monitoring, *Biosens. Bioelectron.*, **2006**, 21, 1405–1423.
7. Chang, T.-S., An Updated Review of Tyrosinase Inhibitors, *Int. J. Mol. Sci.*, **2009**, 10, 2440–2375.
8. Lineweaver, H.; Burk, D., The Determination of Enzyme Dissociation Constants, *JACS*, **1934**, 56, 658–666.
9. Van Boekel, M.A.J.S., Kinetic Modeling of Food Quality: A Critical Review, *CRFSFS*, **2008**, 7, 144–158.
10. Nahorski, S.R.; Ragan, I.; Challiss, R.A.J., Lithium and the Phosphoinositide Cycle: An Example of Uncompetitive Inhibition and its Pharmacological Consequences, *TIPS*, **1991**, 12, 297–303.
11. Schmid, F.-X., Biological Macromolecules: UV-visible Spectrophotometry, *Encyclopedia of Life Sciences*; Macmillan Publishers Ltd, **2001**
12. Flurkey, W.J.; Inlow, J.K., Use of Mushroom Tyrosinase to Introduce Michaelis-Menten Enzyme Kinetics to Biochemistry Students, *Biochem. Mol. Biol. Educ.*, **2017**, 45, 270–276.
13. Friedman, M.E.; Daron, H.H., Tyrosinase An Introductory Experiment with Enzymes, *J. Chem. Ed.*, **1977**, 54, 256.
14. Kanteev, M.; Goldfeder, M.; Fishman, A, Structure-Function Correlations in Tyrosinases, *Protein Sci.*, **2015**, 24, 1360–1369.

Learn more at **thermofisher.com/evolution**

thermo scientific

For research use only. Not for use in diagnostic procedures. For current certifications, visit thermofisher.com/certifications
© 2023 Thermo Fisher Scientific Inc. All rights reserved. All trademarks are the property of Thermo Fisher Scientific and its subsidiaries unless otherwise specified. AN56399_EN 03/23